

Density Level Sets: Asymptotics, Inference, and Visualization

Yen-Chi Chen*

Department of Statistics, University of Washington
and

Christopher R. Genovese[†]

Department of Statistics, Carnegie Mellon University
and

Larry Wasserman[‡]

Department of Statistics, Carnegie Mellon University

September 6, 2016

Abstract

We study the plug-in estimator for density level sets under Hausdorff loss. We derive asymptotic theory for this estimator, and based on this theory, we develop two bootstrap confidence regions for level sets. We introduce a new technique for visualizing density level sets, even in multidimensions, that is easy to interpret and efficient to compute.

Keywords: Nonparametric inference, asymptotic theory, level set clustering, anomaly detection, visualization

*Supported by the William S. Dietrich II Presidential Ph.D. Fellowship and DOE grant number DE-FOA-0000918 at Carnegie Mellon University.

[†]Supported by DOE grant number DE-FOA-0000918 and NSF grant number DMS-1208354.

[‡]Supported by NSF grant number DMS-1208354.

1 Introduction

Estimating the level sets of a probability density function has a wide range of applications, including anomaly detection (outlier detection) (Breunig et al., 2000; Hodge and Austin, 2004), two-sample comparison (Duong et al., 2009), binary classification (Mammen and Tsybakov, 1999), and clustering (Rinaldo and Wasserman, 2010; Rinaldo et al., 2012). In this paper, we study the problem of estimating the level set

$$D_h \equiv D_h(\lambda) = \{x : p_h(x) = \lambda\}, \quad (1)$$

where p_h is the expected kernel density estimator with bandwidth h , a smoothed version of the underlying density p . Using D_h (and thus p_h) has several advantages, which we discuss in detail in Section 2.2. Figures 5 and 10 illustrate the kind of confidence sets and visualizations we will develop in this paper.

A commonly used estimator of the density level-set is the plug-in estimator $\widehat{D}_h = \{x : \widehat{p}_h(x) = \lambda\}$, where \widehat{p}_h is the kernel density estimator or some other density estimator. There is a large literature for level sets (and upper level sets, which replace $= \lambda$ with $\geq \lambda$) that focuses on the consistency, rates of convergence (Polonik, 1995; Tsybakov, 1997; Walther, 1997; Cadre, 2006; Cuevas et al., 2006) and minimaxity (Singh et al., 2009) of such estimators under various error loss functions.

Recent results on statistical inference for level sets include Jankowski and Stanberry (2012) and Mammen and Polonik (2013). Statistical inference is challenging in this setting because the estimand is a set and the estimator is a random set (Molchanov, 2005). Mason and Polonik (2009) establish asymptotic normality for upper level sets when the loss function is the measure of the set difference. However, it is unclear how to derive a confidence set from this result.

Another challenge of level set estimation is that we cannot directly visualize the level sets when the dimension of the data d is larger than 3. One approach is to construct a *level-set tree*, which shows how the connected components for the upper level sets bifurcate when we gradually increase λ (Stuetzle, 2003; Klemelä, 2004, 2006, 2009; Stuetzle and Nugent, 2010; Kent et al., 2013). The level-set tree reveals topological information about the level sets but loses geometric information.

In this paper, we propose solutions to all of these problems. Our main contributions can be summarized as follows.

1. We derive the limiting distribution of $\text{Haus}(\widehat{D}_h, D_h)$ (Theorem 3).
2. We develop two bootstrap-based methods to construct confidence regions for D_h (Section 4).
3. We prove that both bootstrap methods are valid (Theorem 4 and 5).
4. We devise a visualization technique that preserves the geometric information for density level sets (Section 5).

Related Work. Early work on density level set focuses on proving the consistency or the rate of convergence under various metrics. See e.g. Polonik (1995); Tsybakov (1997); Walther (1997); Cuevas et al. (2006); Rinaldo and Wasserman (2010). However, none of these derives a limiting distribution for the density level sets. To our knowledge, the only paper that considers limiting distributions is Mason and Polonik (2009), proving asymptotic normality under a generalized integrated distance. However, this metric cannot be used to construct a confidence set for density level sets since the asymptotic distribution involves the true density, which is unknown. Estimating the level set is also related to support estimation, see e.g. Cuevas and Rodríguez-Casal (2004) and Cuevas (2009).

Jankowski and Stanberry (2012) and Mammen and Polonik (2013), both provide methods for constructing confidence sets for the density level sets using the variation of the density function. Our approach is similar to theirs but is based on Hausdorff distance. We will compare their methods to ours in Section 4.2.

Outline. We begin with a short introduction to density level sets along with some useful geometric concepts in Section 2. In Section 3, we derive the limiting distribution of the Hausdorff distance between the estimated and true level sets. In Section 4, we construct a valid confidence set for density level sets. In Section 5, we devise a visualization method for density level sets that is simple to interpret and efficient to compute. (We provide an R package that implements our visualization method.) We summarize our results and discuss related problems in Section 6.

2 Technical Background

2.1 Level Sets

Let X_1, \dots, X_n be a random sample from an unknown, continuous density $p(x)$. We define the density level set by

$$D \equiv D(\lambda) = \{x : p(x) = \lambda\} \quad (2)$$

for some $\lambda > 0$. Note that in the literature the term level sets is sometimes used for the set $\{x : p(x) \geq \lambda\}$; we call the latter the *upper level set* to distinguish it from the *level set* in equation 2. Thus, the level sets (in our terminology) are the boundaries to the upper level sets, under mild smoothness assumptions (e.g., assumption G below).

We assume that λ is a fixed, positive value. A plug-in estimate for D is

$$\widehat{D}_h \equiv \widehat{D}_h(\lambda) = \{x : \widehat{p}_h(x) = \lambda\}, \quad (3)$$

where \widehat{p}_h is the kernel density estimator (KDE),

$$\widehat{p}_h(x) = \frac{1}{nh^d} \sum_{i=1}^n K\left(\frac{\|x - X_i\|}{h}\right). \quad (4)$$

2.2 Smoothed Density Level Set

In this paper, we focus on inference for the level sets of a smoothed version of p , specifically:

$$p_h = p \star K_h = \mathbb{E}(\widehat{p}_h), \quad (5)$$

where $K_h(x) = \frac{1}{h^d} K\left(\frac{\|x\|}{h}\right)$ and \star denotes convolution. We denote the λ level set of p_h by

$$D_h = \{x : p_h(x) = \lambda\}. \quad (6)$$

Note that although we focus on estimating D_h , we allow $h = h_n \rightarrow 0$ as $n \rightarrow \infty$.

Here, we argue that p_h (and hence D_h) is a better target for level-set estimation than p (and hence D). For simplicity, in this section we focus on the upper level sets $L_h(\lambda) = \{x : p_h(x) \geq \lambda\}$ and $L(\lambda) = \{x : p(x) \geq \lambda\}$, but the gist of the argument remains the same in either case.

Our arguments are: (i) p_h always exists while p may not even exist; (ii) \widehat{p}_h can

be naturally viewed as an estimator for p_h ; (iii) p_h has all the salient structure of p but is easier to estimate than p ; (iv) While the bias $p_h(x) - p(x)$ may be analyzed theoretically, in practice, it cannot be accurately estimated. It is better to just be clear that we are really estimating p_h .

Let us now expand on some of these points. Regarding point (ii): Let X_1, \dots, X_n be an iid sample from P , where P is supported on some compact set $\mathbb{K} \subset \mathbb{R}^d$. We have, for any P ,

$$P^n \left(\sup_x |\hat{p}_h(x) - p_h(x)| \geq \epsilon \right) \leq c_1 e^{-c_2 n h^d \epsilon^2}.$$

As long as $h \geq (\log n/n)^{1/d}$, $P^n(\sup_x |\hat{p}_h(x) - p_h(x)| \geq \epsilon) \rightarrow 0$, and hence we can uniformly consistently estimate p_h , whether we keep h fixed or let it tend to 0. The same is *not* true for p . In fact, P may not even have a density p . The bias cannot be uniformly estimated in a distribution-free way.

Regarding (iii): The left plot in Figure 1 shows a density p . The blue points at the bottom show the upper level set $L = \{x : p \geq 0.05\}$. The right plot shows p_h for $h = 0.2$ and the blue points at the bottom show the upper level set $L_h = \{x : p_h \geq 0.05\}$. The smoothed out density p_h is biased and the upper level set L_h loses the small details of L . But these small details are the least estimable, and L_h captures the principal structure of L . In addition, when L is smooth (having positive μ -reach; Chazal and Lieutier 2005; Chazal et al. 2009) and h is sufficiently small, L_h and L will be topologically similar, in the sense that a small expansion of L_h is homotopic to L (Chazal and Lieutier 2005; Chazal et al. 2009; Genovese et al. 2014). The μ -reach and the concept of being nearly homotopic can be found in section 3.2 of Genovese et al. (2014) and section 4 of Chazal et al. (2009).

As a second example, let $P = (1/3)\phi(x; -5, 1) + (1/3)\delta_0 + (1/3)\phi(x; 5, 1)$ where ϕ is a Normal density and δ_0 is a point mass at 0. Of course, this distribution does not even have a density. The left plot in Figure (2) shows the density of the absolutely continuous part of P with a vertical line to who the point mass. The right plot shows p_h , which is a smooth, well-defined density. Again the blue points show the level sets. As before p_h and L_h are slightly biased, but they are also well-defined. And \hat{p}_h and \hat{L}_h are accurate estimators of p_h and L_h , respectively. Moreover, L_h captures the most important qualitative information about L , namely, that there are three connected components, one of which is small. These examples show that p_h — and hence D_h

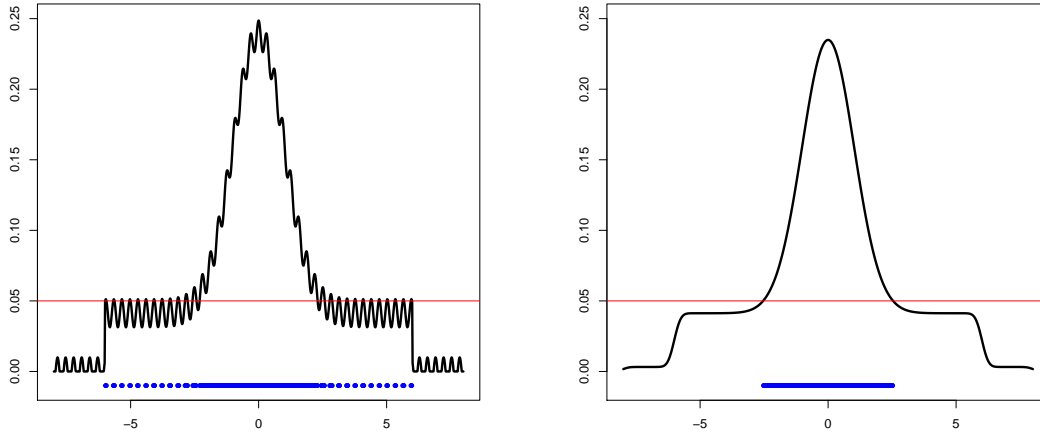


Figure 1: Left: a density p and an upper level set $\{p \geq t\}$. Right: the smoothed density p_h and the upper level set $\{p_h \geq t\}$.

— is a sensible target of inference.

Lastly, we would like to point out that the idea of viewing p_h as the estimand is not new. The “scale space” approach to smoothing explicitly argues that we should view \hat{p}_h as an estimate of p_h , and p_h is then regarded as a view of p at a particular resolution. This idea is discussed in detail in [Chaudhuri et al. \(2000\)](#); [Chaudhuri and Marron \(1999\)](#); [Godtliebsen et al. \(2002\)](#).

If one really wants to focus on making inference for D , the level set of the original density, then we need to undersmooth¹ so that the bias will not affect the limiting distribution. This leads to estimates of D that are highly variable. We believe that an accurate confidence set for D_h is more useful than a poor confidence set for D .

Remark 1. These arguments explain why we regard p_h rather than p as the estimand. But these arguments do not tell us how to choose h . Bandwidth selection is always a challenge and in this paper we mainly use Silverman’s rule of thumb ([Silverman \(1986\)](#)).

¹Undersmoothing the density estimate to make statistical inferences is a common practice in nonparametric statistics; see e.g. page 89 of [Wasserman \(2006\)](#).

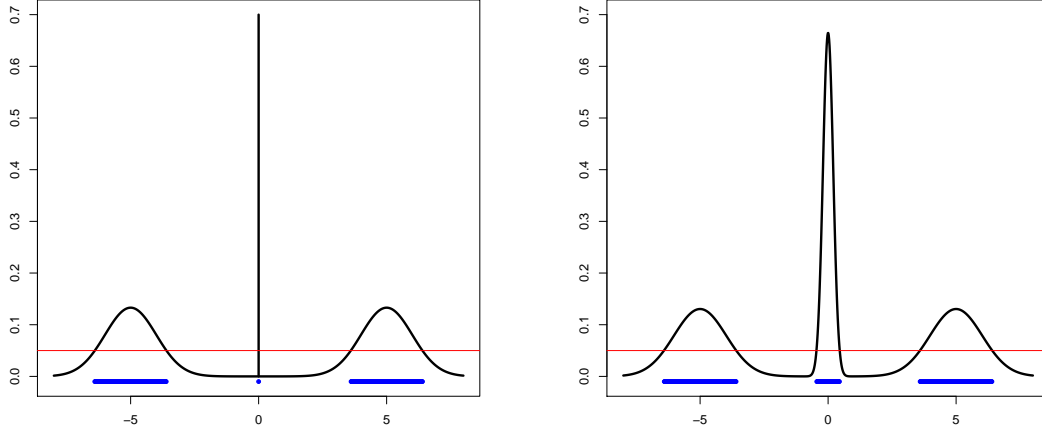


Figure 2: Left: a distribution with a continuous component and a point mass at 0. Right: the smoothed density p_h . The upper level set L_h is biased but is estimable and it approximates the main features of L .

2.3 Geometric Concepts

Let $\pi_A(x)$ be the *projection* of a point x onto a set A . Note that $\pi_A(x)$ may not be unique. The distance induced by the projection is

$$d(x, A) = \inf\{\|x - y\|_2 : y \in A\} = \|x - \pi_A(x)\|_2 \quad (7)$$

A common measure of distance between two subsets of a metric space (e.g., \mathbb{R}^d) is the *Hausdorff distance*, given by

$$\begin{aligned} \text{Haus}(A, B) &= \inf\{\epsilon : A \subset B \oplus \epsilon \text{ and } B \subset A \oplus \epsilon\} \\ &= \max\left\{\sup_{x \in B} d(x, A), \sup_{x \in A} d(x, B)\right\}, \end{aligned} \quad (8)$$

where $A \oplus \epsilon = \bigcup_{x \in A} B(x, \epsilon)$ and $B(x, \epsilon) = \{y : \|x - y\| \leq \epsilon\}$. The Hausdorff distance is a generalized version of the \mathcal{L}_∞ metric for sets.

The *reach* of a set M (Federer 1959; Cuevas 2009, also known as condition number Niyogi et al. 2008 or minimal feature size Chazal and Lieutier 2005) is the largest distance from M such that every point within this distance to M has a unique projection onto M . i.e.

$$\text{reach}(M) = \sup\{r : \pi_M(x) \text{ is unique } \forall x \in M \oplus r\}. \quad (9)$$

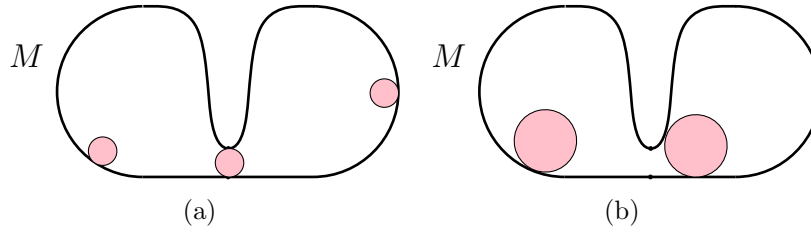


Figure 3: An illustration for reach. The reach is the largest radius for a ball that can freely move along the set M . In (a), the radius of the pink ball is equal to the reach. In (b), the radius is too large so that it cannot pass the small gap on M .

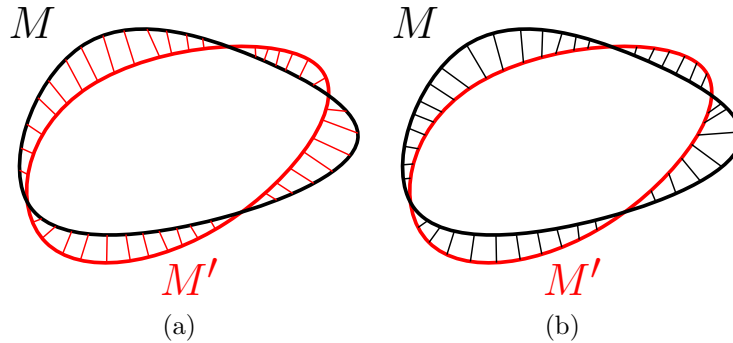


Figure 4: An example for two normal compatible curves. Panel (a): each thin red line indicates the projection from a point of M onto M' . Panel (b): each thin black line indicates the projection from a point of M' onto M . When these projections are one to one and onto, we say M and M' are normal compatible to each other.

Note that $\pi_A(x)$ is unique if $0 < d(x, A) \leq \text{reach}(A)$. Another way to understand the reach is as the largest radius of a ball that can freely move along M ; see Figure 3 for an example. In some cases, the reach is the same as the smallest radius of curvature on M . The reach plays a key role in relating the Hausdorff distance to the empirical process. Note that the reach is closely related to ‘rolling properties’ and ‘ α -convexity’; see Cuevas (2009), Cuevas et al. (2012) and appendix A of Pateiro-López (2008).

Finally, two smooth sets A and B are called *normal compatible* (Chazal et al., 2007) if the projection between A and B are one to one and onto; see Figure 4 for an example. When A and B are normal compatible, the Hausdorff distance has the simpler form

$$\text{Haus}(A, B) = \sup_{x \in B} d(x, A) = \sup_{x \in A} d(x, B). \quad (10)$$

3 Asymptotic Theory

In this section, we derive the asymptotic theory for $\text{Haus}(\widehat{D}_h, D_h)$. Note first that for two sets A and B , the Hausdorff distance satisfies the inclusion property

$$A \subset B \oplus \text{Haus}(A, B), \quad B \subset A \oplus \text{Haus}(A, B). \quad (11)$$

From this, it follows that when we have a set estimator \widehat{A}_n and a parameter of interest A , then for any $\alpha > 0$, the set

$$\widehat{A}_n \oplus \text{Quantile}\left(\text{Haus}(\widehat{A}_n, A), 1 - \alpha\right) \quad (12)$$

is a $1 - \alpha$ confidence set for A , where $\text{Quantile}(X, \alpha)$ is the α -quantile of random variable X . Thus, whenever we can approximate the distribution of $\text{Haus}(\widehat{A}_n, A)$, we can construct a confidence set for A . Note that [Chen et al. \(2014b\)](#) and [Chen et al. \(2014a\)](#) have used this property to construct confidence sets, but neither paper used this property to full effect.

We now define some notation that will be used throughout this paper. Let \mathbf{BC}^r denote the collection of functions (including both univariate and multivariate functions) with bounded continuous derivatives up to the r -th order. For a smooth function $f : \mathbb{R}^d \mapsto \mathbb{R}$ with $f \in \mathbf{BC}^r$, we denote the elementwise max norm for r -th derivative as $\|f\|_{r, \max}$. For instance,

$$\|f(x)\|_{1, \max} = \max_{1 \leq i \leq d} \left| \frac{\partial f(x)}{\partial x_i} \right|, \quad \|f(x)\|_{2, \max} = \max_{1 \leq i, j \leq d} \left| \frac{\partial^2 f(x)}{\partial x_i \partial x_j} \right|.$$

We define the sup norm using derivatives up to r -th order by:

$$\|f\|_{r, \max}^* = \max \left\{ \sup_{x \in \mathbb{K}} \|f(x)\|_{\ell, \max} : \ell = 0, \dots, r \right\}. \quad (13)$$

Let $\alpha = (\alpha_1, \dots, \alpha_d)$ be a multi-index such that each α_j is a non-negative integer and $|\alpha| = \alpha_1 + \dots + \alpha_d$. We define

$$f^{(\alpha)} = \frac{\partial^{|\alpha|}}{\partial^{\alpha_1} x_1 \dots \partial^{\alpha_d} x_d} f(x)$$

to be the partial derivative. Note that for a vector $v \in \mathbb{R}^d$, the norm $\|v\|$ denotes the usual Euclidean norm. Throughout this paper, we use the conventional notation for

$O_P(\cdot)$ and $O(\cdot)$ for $n \rightarrow \infty$ and $h = h_n$, where possibly $h_n \rightarrow 0$.

We now state the main assumptions, for an arbitrary density q . When we use the assumptions in what follows, we will take q to be p_h .

Assumptions.

(G) Let $D(q) = \{x \in \mathbb{K} : q(x) = \lambda\}$ be the level set for a density q . There are $\delta_0, g_0 > 0$ such that $\forall x \in D(q) \oplus \delta_0$, we have $\|\nabla q(x)\| > g_0$.

(K1) The kernel function $K \in \mathbf{BC}^3$ and is symmetric, non-negative, and

$$\int x^2 K^{(\alpha)}(x) dx < \infty, \quad \int (K^{(\alpha)}(x))^2 dx < \infty$$

for all multi-indices α satisfying $|\alpha| \leq 3$.

(K2) The kernel function K and its partial derivative satisfies condition K_1 in [Giné and Guillou \(2002\)](#). Specifically, let

$$\mathcal{K} = \left\{ y \mapsto K^{(\alpha)} \left(\frac{x-y}{h} \right) : x \in \mathbb{R}^d, h > 0, |\alpha| \leq 2 \right\} \quad (14)$$

We require that \mathcal{K} satisfies

$$\sup_P N(\mathcal{K}, L_2(P), \epsilon \|F\|_{L_2(P)}) \leq \left(\frac{A}{\epsilon} \right)^v \quad (15)$$

for some positive numbers A and v , where $N(T, d, \epsilon)$ denotes the ϵ -covering number of the metric space (T, d) , F is the envelope function of \mathcal{K} , and the supremum is taken over the whole \mathbb{R}^d . The A and v are usually called the VC characteristics of \mathcal{K} . The norm $\|F\|_{L_2(P)}^2 = \int |F(x)|^2 dP(x)$.

Assumption (G) appears in [Molchanov \(1991\)](#); [Tsybakov \(1997\)](#); [Walther \(1997\)](#); [Molchanov \(1998\)](#); [Cadre \(2006\)](#); [Mammen and Polonik \(2013\)](#); [Laloe and Servien \(2013\)](#). For a smooth density q , (G) holds whenever the specified level λ does not coincide with the density value for a critical point.

Assumption (K1) is to guarantee that the variance of the KDE is bounded and to ensure that $p_h \in \mathbf{BC}^3$. This assumption is very common in statistical literature, see e.g. [Wasserman \(2006\)](#). Assumption (K2) is to regularize the complexity of the kernel function so that the supremum norm for kernel functions and their derivatives can be bounded in probability. Similar assumption appears in [Einmahl and Mason \(2005\)](#)

and [Genovese et al. \(2014\)](#). The Gaussian kernel and many compactly supported kernels satisfy both assumptions.

An immediate result from assumption (G) is the smoothness of the density level set. This smoothness property will be used to understand the distribution of $\text{Haus}(\widehat{D}_h, D_h)$.

Lemma 1 (Smoothness Theorem). *Assume a density $p_h \in \mathbf{BC}^2$ satisfies condition (G) and let D_h denote the level set for p_h at λ . Then*

$$\text{reach}(D_h) \geq \min \left\{ \frac{\delta_0}{2}, \frac{g_0}{\|p_h\|_{2,\max}^*} \right\}. \quad (16)$$

Moreover, let $q \in \mathbf{BC}^3$ be another density function and define $D(q)$ as the level set for q at level λ . When $\|p_h - q\|_{2,\max}^*$ is sufficiently small,

1. Condition (G) holds for q .
2. $\text{reach}(D(q)) = \min \left\{ \frac{\delta_0}{2}, \frac{g_0}{\|p_h\|_{2,\max}^*} \right\} + O(\|p_h - q\|_{2,\max}^*)$.
3. D_h and $D(q)$ are normal compatible.

The proof is given in the supplementary materials. Lemma 1 is very similar to Theorem 1 and 2 in [Walther \(1997\)](#). Essentially, this lemma shows that the level set D is smooth and that whenever two smooth densities are sufficiently close, their level sets will both be smooth, be close to each other, and have one-to-one and onto normal projections between them.

Given a collection of functions $\mathcal{F} = \{f_t : \mathbb{R}^d \mapsto \mathbb{R} : t \in T\}$, where T is some index set, the empirical process \mathbb{G}_n is defined as

$$\mathbb{G}_n(f) = \frac{1}{\sqrt{n}} \sum_{i=1}^n (f(X_i) - \mathbb{E}(f(X_1))), \quad f \in \mathcal{F}. \quad (17)$$

Lemma 2 (Empirical Approximation). *Assume (K1–K2) and (G) hold for p_h . Let D_h and \widehat{D}_h be the density level sets with level λ for p_h and \widehat{p}_h . Define the function*

$$f_x(y) = \frac{1}{\sqrt{h^d} \|\nabla p_h(x)\|} K \left(\frac{x-y}{h} \right) \quad (18)$$

with $x \in D_h$. If $\frac{\log n}{nh^{d+2}} \rightarrow 0$, $h \rightarrow 0$, then

$$\sup_{x \in D_h} \left| \frac{\mathbb{G}_n(f_x) - \sqrt{nh^d} \cdot d(x, \widehat{D}_h)}{\sqrt{nh^d} \cdot d(x, \widehat{D}_h)} \right| = O(\|\widehat{p}_h - p_h\|_{1,\max}^*) = O_P \left(\sqrt{\frac{\log n}{nh^{d+2}}} \right). \quad (19)$$

A key element for the proof of Lemma 2 is the smoothness of D_h and \widehat{D}_h , which relies on Lemma 1. This smoothness allows us to approximate the local difference by an empirical process.

Remark 2. Lemma 2 implies that for each $x \in D_h$, $d(x, \widehat{D}_h)$ converges to a mean 0 Gaussian process. We can use $\mathbb{E} \left(d(x, \widehat{D}_h)^2 \right)$ as a measure of *local uncertainty* Chen et al. (2014b) – analogous to the mean squared error – and thus can apply the bootstrap to estimate this quantity.

Lemma 2 shows that the projected distance to the level sets can be approximated by a stochastic process (the empirical process) defined on a smooth manifold. Specifically, Lemma 2 shows that the projection distance can be approximated by an empirical process on certain functions f_x , where $x \in D_h$. The level sets D_h now acts as an index set. Thus, we define the function space

$$\mathcal{F} = \left\{ f_x(y) \equiv \frac{1}{\sqrt{h^d} \|\nabla p_h(x)\|} K \left(\frac{x-y}{h} \right) : x \in D_h \right\} \quad (20)$$

and define a Gaussian process \mathbb{B} on \mathcal{F} such that for all $f_1, f_2 \in \mathcal{F}$,

$$\mathbb{B}(f_1) \stackrel{d}{=} N(0, \mathbb{E}(f_1(X_1)^2)), \quad \text{Cov}(\mathbb{B}(f_1), \mathbb{B}(f_2)) = \mathbb{E}(f_1(X_1)f_2(X_1)). \quad (21)$$

Theorem 3 (Asymptotic Theory). *Assume (K1–K2) and (G) holds for p_h . Let D_h and \widehat{D}_h be the density level sets with level λ for p_h and \widehat{p}_h . Then when $\frac{\log n}{nh^{d+2}} \rightarrow 0$, $h \rightarrow 0$, the Hausdorff distance satisfies*

$$\sup_t \left| \mathbb{P} \left(\sqrt{nh^d} \text{Haus}(\widehat{D}_h, D_h) < t \right) - \mathbb{P} \left(\sup_{f \in \mathcal{F}} |\mathbb{B}(f)| < t \right) \right| = O \left(\left(\frac{\log^7 n}{nh^d} \right)^{1/8} \right), \quad (22)$$

where \mathcal{F} is defined in equation (20) and \mathbb{B} is a Gaussian process defined on \mathcal{F} satisfying equation (21).

The proof of Theorem 3 depends on two geometric observations. First, the empirical approximation in Lemma 2, shows that the local difference is approximately the same as an empirical process, and hence the maximum local difference is approximated by the maximum of the empirical process. Second, the normal compatibility between \widehat{D}_h and D_h guaranteed by Lemma 1, which implies that maximal of local difference is the same as the Hausdorff distance.

Theorem 3 shows that the Hausdorff distance $\text{Haus}(\widehat{D}_h, D_h)$ can be approximated by a maximum over a certain Gaussian process. Note that we cannot directly use this theorem to construct a confidence set for D_h since the Gaussian process is defined on D_h , which is unknown. Later we will use the bootstrap to approximate this limiting distribution and construct a confidence set.

The random variable $\sup_{f \in \mathcal{F}} |\mathbb{B}(f)|$ follows an extreme-value type distribution. However, writing down the explicit form for this distribution is not very helpful in statistical inference because it involves unknown quantities and because the convergence to the distribution is notoriously slow. Instead, we will use the bootstrap to approximate the distribution of $\text{Haus}(\widehat{D}_h, D_h)$, avoiding the unknown quantities and yielding much faster convergence.

4 Statistical Inference

We now show that we can construct valid confidence sets for D_h with the bootstrap. A set $S_{n,1-\alpha}$ is called an asymptotically valid confidence set for D_h if

$$\mathbb{P}(D_h \subset S_{n,1-\alpha}) = 1 - \alpha + O(r_n), \quad (23)$$

where $r_n \rightarrow 0$ as $n \rightarrow \infty$. We propose two methods for constructing a confidence set, and we will show that they are both asymptotically valid.

4.1 Method 1: Hausdorff Loss

The first approach is to use the Hausdorff distance between the level sets. Let $W_n = \text{Haus}(\widehat{D}_h, D_h)$ and define

$$w_{1-\alpha} = F_{W_n}^{-1}(1 - \alpha), \quad (24)$$

where F_A denotes the cdf for a random variable A . Then, it is easy to see that

$$\mathbb{P}(D_h \subset \widehat{D}_h \oplus w_{1-\alpha}) \geq 1 - \alpha. \quad (25)$$

We use the bootstrap to estimate $w_{1-\alpha}$.

Let X_1^*, \dots, X_n^* be a bootstrap sample from the empirical measure. Let \widehat{p}_h^* denote the KDE using the bootstrap sample, and \widehat{D}_n^* the corresponding level set. We define

$W_n^* = \text{Haus}(\widehat{D}_n^*, \widehat{D}_h)$ and

$$\widehat{w}_{1-\alpha} = F_{W_n^*}^{-1}(1 - \alpha), \quad (26)$$

Then the bootstrap confidence set is $\widehat{D}_h \oplus \widehat{w}_{1-\alpha}$.

Theorem 4. *Assume (K1–K2) and (G) holds for p_h and $\frac{\log n}{nh^{d+2}} \rightarrow 0$, $h \rightarrow 0$. Let D_h and \widehat{D}_h and \widehat{D}_n^* be the density level set with level λ for p_h and \widehat{p}_h and \widehat{p}_h^* . Then there exist \mathcal{X}_n such that*

$$\begin{aligned} \sup_t \left| \mathbb{P} \left(\sqrt{nh^d} \text{Haus} \left(\widehat{D}_n^*, \widehat{D}_h \right) < t \mid X_1, \dots, X_n \right) - \mathbb{P} \left(\sqrt{nh^d} \text{Haus}(\widehat{D}_h, D_h) < t \right) \right| \\ = O \left((\|\widehat{p}_h - p_h\|_{\max})^{1/8} \right) \end{aligned} \quad (27)$$

for all $(X_1, \dots, X_n) \in \mathcal{X}_n$ and $\mathbb{P}(\mathcal{X}_n) \geq 1 - 3e^{-nh^{d+2}\tilde{A}_0}$ for some constants \tilde{A}_0 . Thus,

$$\mathbb{P} \left(D_h \subset \widehat{D}_h \oplus \widehat{w}_{1-\alpha} \right) = 1 - \alpha + O \left(\left(\frac{\log^7 n}{nh^d} \right)^{1/8} \right). \quad (28)$$

An intuitive explanation for Theorem 4 is that as n goes to infinity, the bootstrap process converges to the same Gaussian process as the empirical process – thus, they share the same Berry-Esseen bound.

4.2 Method 2: Supremum Loss

The second approach is to use the supremum norm of the KDE and impose an upper and lower bound around the density level.

Let $M_n = \sup_{x \in \mathbb{K}} |\widehat{p}_h(x) - p_h(x)|$ and $m_{1-\alpha} = F_{M_n}^{-1}(1 - \alpha)$. Define

$$C_{n,1-\alpha} = \{x \in \mathbb{K} : |\widehat{p}_h(x) - \lambda| \leq m_{1-\alpha}\}. \quad (29)$$

It is easy to verify that

$$\mathbb{P}(D_h \subset C_{n,1-\alpha}) \geq 1 - \alpha. \quad (30)$$

Again we use the bootstrap to estimate the quantile. Recall that \widehat{p}_h^* is the KDE based on the bootstrap sample. We define $M_n^* = \sup_{x \in \mathbb{K}} |\widehat{p}_h^*(x) - \widehat{p}_h(x)|$ and set

$$\widehat{m}_{1-\alpha} = F_{M_n^*}^{-1}(1 - \alpha). \quad (31)$$

Then the confidence set is

$$\widehat{C}_{n,1-\alpha} = \{x \in \mathbb{K} : |\widehat{p}_h(x) - \lambda| \leq \widehat{m}_{1-\alpha}\}. \quad (32)$$

Theorem 5. *Assume (K1–K2) and (G) holds for p_h and $\frac{\log n}{nh^{d+2}} \rightarrow 0$, $h \rightarrow 0$. Let D_h and \widehat{D}_h and \widehat{D}_n^* be the density level sets with level λ for p_h and \widehat{p}_h and \widehat{p}_h^* . Then*

$$\mathbb{P}\left(D_h \subset \widehat{C}_{n,1-\alpha}\right) = 1 - \alpha + O\left(\left(\frac{(\log^7 n)}{nh^d}\right)^{1/8}\right).$$

The proof of this Theorem is similar to the proof of Theorem 4, so we omit the details. The basic idea is as follows. By equation (30), the quantile of \widehat{M}_n can be used to construct confidence sets. We then show that $\sqrt{nh^d}M_n$ is approximated by the maximum of a Gaussian process (similar to Theorem 3 and made explicit in Chernozhukov et al. 2014a). Finally, we show that the bootstrap $\sqrt{nh^d}M_n^*$ converges to $\sqrt{nh^d}M_n$ as in Theorem 4.

This method embodied in Theorem 5 is very similar to the methods in Jankowski and Stanberry (2012) and Mammen and Polonik (2013). Jankowski and Stanberry (2012) proposes to construct a confidence set of the form

$$C_n = \{x : \lambda - \ell_n \leq \widehat{p}_h(x) \leq \lambda + \tau_n\} \quad (33)$$

with some $\ell_n, \tau_n \rightarrow 0$. They require that $\sqrt{nh^d}(\widehat{p}_h - p_h)$ converges weakly to a known random field. This convergence is true when h is fixed but is *not* attainable if we allow $h = h_n \rightarrow 0$, in contrast to our approach, which supports both cases. They also assume the limiting random field is either known or can be easily estimated; we do not require that assumption.

Mammen and Polonik (2013) construct a confidence set using a similar approach to method 2, but they focus on the original level set $D = \{x : p(x) = \lambda\}$ rather than the smoothed version D_h . Instead of taking the supremum of the density deviation over the whole support \mathbb{K} , they propose to focus on the regions $x \in D \Delta \widehat{D}_h$. i.e.

$$R_n = \sup_{x \in D \Delta \widehat{D}_h} |\widehat{p}_h(x) - p|, \quad (34)$$

where $A \Delta B = \{x : x \in A, x \notin B\} \cup \{x : x \in B, x \notin A\}$ is the symmetric difference

between sets. Then they use the upper quantile of R_n to construct a confidence set of a similar form to (29) and apply the bootstrap to estimate the quantile. Their bootstrap consistency relies on Neumann’s method (Proposition 3.1 in Neumann (1998)) and they assume that h converges fast enough so that one can ignore the bias for estimating the original density p . Actually, under their assumptions, our proposed bootstrap confidence sets (from both methods 1 and 2) are also consistent for the original level set D since the bias converges faster than the stochastic variation. The method in Mammen and Polonik (2013) should have higher power than our method 2 since they consider taking the supremum over a smaller region.

Remark 3. We may use a variance stabilizing transform to obtain an adaptive confidence set using similar idea to Chernozhukov et al. (2012). The variance of $\widehat{p}_h(x)$ is proportional to $p(x)$. Thus, we may use

$$V_n^* = \sup_{x \in \mathbb{K}} \frac{|\widehat{p}_h^*(x) - \widehat{p}_h(x)|}{\sqrt{\widehat{p}_h(x)}} \quad (35)$$

$$\widehat{v}_{1-\alpha} = F_{V_n^*}^{-1}(1 - \alpha) \quad (36)$$

and set $\widehat{v}_{1-\alpha} \times \sqrt{\widehat{p}_h(x)}$ as an adaptive threshold for constructing the confidence set. Namely, the adaptive confidence set is given by

$$\widehat{C}_{n,1-\alpha}^* = \left\{ x \in \mathbb{K} : |\widehat{p}_h(x) - \lambda| \leq \widehat{v}_{1-\alpha} \times \sqrt{\widehat{p}_h(x)} \right\}. \quad (37)$$

Using the same approach as in the proof to Theorem 5, we can show that $\widehat{C}_{n,1-\alpha}^*$ has asymptotically $1 - \alpha$ coverage.

Remark 4. The rate $O\left(\left(\frac{\log^7 n}{nh^d}\right)^{1/8}\right)$ may not be optimal. In Chernozukov et al. (2014), they apply a induction technique that gives a rate of order $n^{-1/6}$ for the Gaussian approximation. Despite not being mentioned explicitly in that paper, we believe that similar technique applies to the empirical process. If this is true, the rate in Theorem 3, 4 and 5 can be further refined to $O\left(\left(\frac{\log^7 n}{nh^d}\right)^{1/6}\right)$.

4.3 Comparing Methods 1 and 2

Both methods 1 and 2 generate confidence sets with asymptotically valid coverage. Figure 5 compares the 90% confidence sets from both methods on the old faithful dataset. Apparently, method 1 (left panel; blue regions) is superior to method 2 (right

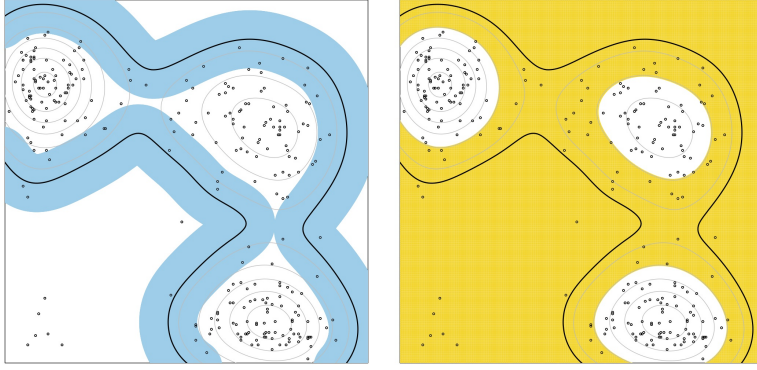


Figure 5: An example of 90% confidence sets using Hausdorff loss of level set (method 1; blue regions in left panel) and the supremum loss of the density (method 2; gold regions in right panel). This dataset is the old faithful dataset. As can be seen easily, the supremum loss of density (right panel) is too huge so that it contains a wide regions as the confidence set. On the other hand, Hausdorff loss of level sets (left panel) gives a much tighter confidence set. The smoothing parameter $h = 0.3$ and the two axes are from 1.5 to 5.5.

panel; gold regions) in the sense that the size of confidence set is much smaller. The main reason is that both methods use the maximum over certain empirical processes but the two processes are defined on different function spaces. Method 1 only takes the supremum over a small function space \mathcal{F} , in which the index set contains only points on the level sets D_h . However, method 2 takes the maximum over a large function space whose index set is the whole space \mathbb{K} . Thus, we expect the second method to have a wider confidence set.

Despite the fact that method 2 yields a much larger confidence sets, it has some nice properties. First, method 2 is very simple: all we need is to compute the bootstrap distribution of supremum loss. Second, method 2 is connected to the methods proposed in [Mammen and Polonik \(2013\)](#) and [Jankowski and Stanberry \(2012\)](#). Third, the confidence sets produced in method 2 are related to level sets with level $\lambda \pm \widehat{m}_{1-\alpha}$. The last property makes it easy to visualize the confidence sets; see [Section 5.3](#).

Here, we consider two simulated datasets to compare the coverage for confidence sets constructed using Hausdorff loss (method 1), L_∞ loss (supremum loss; method 2), and scaled L_∞ loss ([remark 3](#)).

The first dataset is a three-Gaussian mixture. The data is generated from the following distribution:

$$p(x) = \frac{1}{3}\phi_2(x; \mu_1, 0.3^2\mathbf{I}_2) + \frac{1}{3}\phi_2(x; \mu_2, 0.3^2\mathbf{I}_2) + \frac{1}{3}\phi_2(x; \mu_3, 0.3^2\mathbf{I}_2), \quad (38)$$

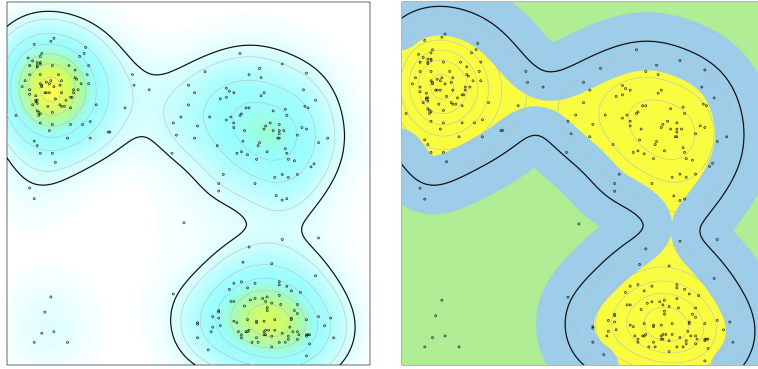


Figure 6: An example for density level sets and confidence regions for the old faithful data. Left: density level set (thick black contour denotes the specified level λ). Right: 90% confidence regions for the density level sets. We also have 90% confidence that (1) all the yellow regions have density above λ (2) all green regions have density below λ and (3) the level sets $\{x : p_h(x) = \lambda\}$ are within the blue regions. Note that the yellow and green regions are the collection of x that we reject $H_{in,0}(x)$ and $H_{out,0}(x)$ and simultaneously control the significance level at $\alpha = 10\%$.

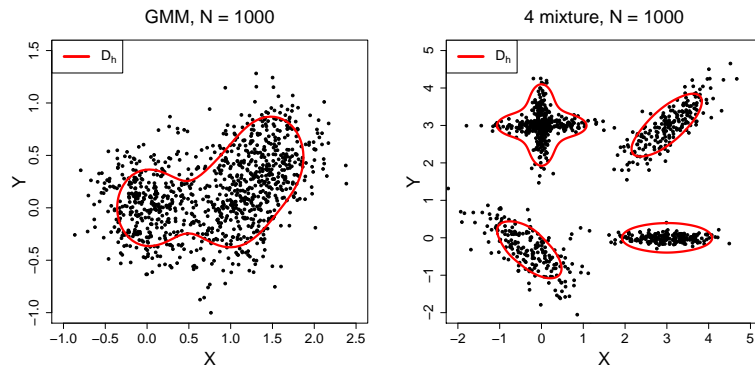


Figure 7: Simulated data for comparing coverage of confidence sets. Left: Three Gaussian mixture dataset. Right: Four-mixture dataset with sample from [Cadre et al. \(2009\)](#). The red curves indicate the density level set we are interested in.

Table 1: Coverage for the three-Gaussian mixture data.

Sample Size	Hausdorff Loss		L_∞ Loss		Scaled L_∞ Loss	
	$\alpha = 0.90$	$\alpha = 0.95$	$\alpha = 0.90$	$\alpha = 0.95$	$\alpha = 0.90$	$\alpha = 0.95$
$n = 500$	0.946	0.983	0.992	0.998	0.957	0.984
$n = 1000$	0.944	0.969	0.991	0.997	0.946	0.974
$n = 2500$	0.915	0.969	0.992	0.998	0.947	0.978

where $\phi_2(x; \mu, \Sigma)$ is the density to bivariate Gaussian with mean vector μ and Covariance matrix Σ . \mathbf{I}_2 is the 2×2 identity matrix and $\mu_1 = (0, 0)^T$, $\mu_2 = (1, 0)^T$, and $\mu_3 = (1.5, 0.5)^T$. We use density level $\lambda = 0.3$ and smoothing parameter $h = 0.2$. The corresponding level set D_h is the red curve in the left panel of Figure 7. We consider three different sample sizes, $N = 500, 1000, 2500$ and compare the coverage of confidence sets using the three methods. The corresponding coverages are given in Table 1. As can be seen from Table 1, all the three methods have the desire nominal coverage.

The second dataset is a four-mixture dataset from Cadre et al. (2009). The data is generated from the following distribution:

$$p(x) = \sum_{\ell=1}^6 \pi_\ell \phi_2(x; \mu_\ell, \Sigma_\ell) \quad (39)$$

with $\pi_1 = \pi_2 = \pi_3 = \pi_4 = 1/5$ and $\pi_5 = \pi_6 = 1/10$, and $\mu_1 = (-0.3, -0.3)^T$, $\mu_2 = (3.0, 3.0)^T$, $\mu_3 = \mu_4 = (0, 3)^T$, $\mu_5 = \mu_6 = (3, 0)$, and

$$\Sigma_1 = \begin{pmatrix} 0.39 & -0.28 \\ -0.28 & 0.39 \end{pmatrix}, \quad \Sigma_2 = \begin{pmatrix} 0.36 & 0.30 \\ 0.30 & 0.36 \end{pmatrix}, \quad (40)$$

$$\Sigma_3 = \Sigma_5 = \begin{pmatrix} 0.33 & 0 \\ 0 & 0.01 \end{pmatrix}, \quad \Sigma_4 = \Sigma_6 = \begin{pmatrix} 0.01 & 0 \\ 0 & 0.33 \end{pmatrix}. \quad (41)$$

We use density level $\lambda = 0.05$ and smoothing parameter $h = 0.2$. The corresponding level set D_h is the red curves in the right panel of Figure 7. Again, we consider three different sample sizes $N = 500, 1000, 2500$ and compare the coverage of confidence sets using the three methods. The corresponding coverages are given in Table 2. It is clear that all the three methods have the desire nominal coverage. Moreover, it can be seen from both Table 1 and 2 that the supremum loss method over covers.

Table 2: Coverage for the four-mixture data.

Sample Size	Hausdorff Loss		L_∞ Loss		Scaled L_∞ Loss	
	$\alpha = 0.90$	$\alpha = 0.95$	$\alpha = 0.90$	$\alpha = 0.95$	$\alpha = 0.90$	$\alpha = 0.95$
$n = 500$	0.991	0.998	1.000	1.000	0.950	0.973
$n = 1000$	0.995	0.998	1.000	1.000	0.917	0.951
$n = 2500$	0.936	0.976	1.000	1.000	0.976	0.991

4.4 Pointwise Hypothesis Tests for Level Sets

The confidence sets developed in the previous section are related to two types of local hypothesis tests. For fixed density level λ and an arbitrary point x , consider the tests of whether $p(x)$ is greater or less than λ :

$$H_{\text{in},0}(x) : p_h(x) \leq \lambda, \quad H_{\text{in},A}(x) : p_h(x) > \lambda, \quad (42)$$

$$H_{\text{out},0}(x) : p_h(x) \geq \lambda, \quad H_{\text{out},A}(x) : p_h(x) < \lambda. \quad (43)$$

When we only want to test just a few points, we can do local tests for each point and control the family-wise error rate to control the type 1 error rate. Usually, however, we are interested conducting the local test at many or even an infinite number of points (like a region), making it difficult to control type 1 error simultaneously.

Inverting the confidence sets of the previous subsection gives a solution to this problem. Let $\widehat{S}_{n,1-\alpha}$ be a confidence set for D_h and let L_h and V_h be, respectively, the upper and lower lambda level sets. Then the decision rules

$$\begin{aligned} T_{\text{in},n}(x) &= 1(\widehat{p}_h(x) \geq \lambda \wedge x \notin \widehat{S}_{n,1-\alpha}), \\ T_{\text{out},n}(x) &= 1(\widehat{p}_h(x) \leq \lambda \wedge x \notin \widehat{S}_{n,1-\alpha}). \end{aligned} \quad (44)$$

control type 1 error simultaneously for all $x \in \mathbb{K}$. This simultaneous control is asymptotic in the sense that $\mathbb{P}(T_{\text{out},n}(x) = 1 \quad \forall x \in L_h) = \alpha + O(r_n)$ for $r_n \rightarrow 0$ and similarly for $T_{\text{in},n}(x)$ and V_h .

In addition, inverting the regions where we cannot reject $H_{\text{in},0}(x)$ and $H_{\text{out},0}(x)$ in (44) yields confidence sets for L_h and V_h . In Figure 6, a 90% confidence regions for the upper level set L_h is the union of yellow and blue regions ($T_{\text{out},n}(x) = 0$). And a 90% confidence regions for V_h , the lower level set, is the union of green and blue regions ($T_{\text{in},n}(x) = 0$). Thus, with 90% confidence, all yellow regions are above λ and the true high density regions should be contained by the yellow and blue regions.

Remark 5. The two local tests described in (42) and (43) are relevant to the problems

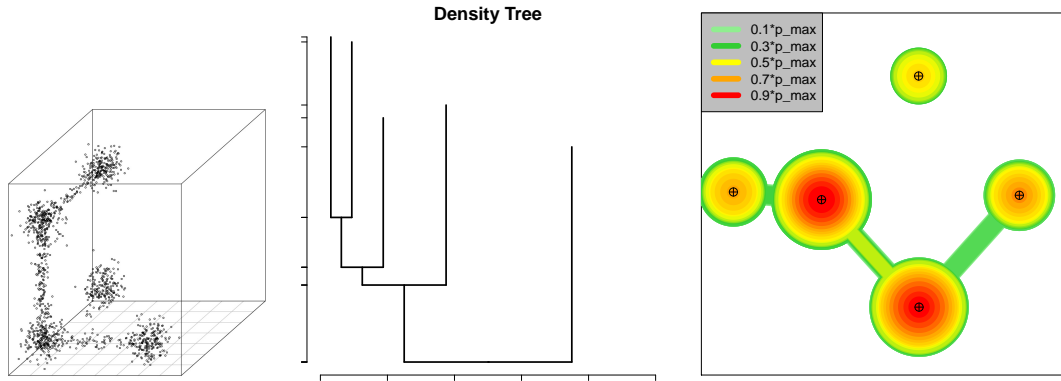


Figure 8: An example for comparing density trees to our visualization method. Left: a 3 dimensional dataset from [Chen et al. \(2014c\)](#). There are 5 clusters and four of them are connected by a tube-like structure. Middle: visualization using the density tree from DeBaCl ([Kent et al., 2013](#)). Right: visualization using our method, which preserves the real connections between clusters. It is easy to see the evolution of multiple level sets and how each cluster is connected to one another using our method. But it is hard to get the same information using density trees.

of level-set clustering ([Hartigan, 1975](#); [Polonik, 1995](#); [Rinaldo and Wasserman, 2010](#); [Rinaldo et al., 2012](#)) and anomaly detection ([Desforges et al., 1998](#); [Breunig et al., 2000](#); [He et al., 2003](#); [Chandola et al., 2009](#)). Rejecting $H_{in,0}(x)$ can be viewed as evidence that x belongs to a level-set cluster. And a point x where $H_{out,0}(x)$ is rejected can be viewed as anomalous.

Remark 6. Note that one can modify the local testing procedure to control the False Discovery Rate ([Benjamini and Hochberg, 1995](#)) rather than familywise error.

5 Visualization for Multivariate Level Sets

Level-set estimators can reveal useful information about a distribution, but beyond three dimensions, we cannot directly visualize the level sets, making the results difficult to use.

In this section, we propose a novel visualization technique density upper level sets in multidimensions. Any visualization entails some loss of information, but our goals are to preserve important geometric information about the sets, make the overall visualization easy to interpret, and give a method that is efficient to compute. Our method exploits the relationship between level-set clustering and mode clustering (see [Figure 9](#)).

A current and commonly used visualization method for level sets is the density tree ([Stuetzle, 2003](#); [Klemelä, 2004, 2006](#); [Kent et al., 2013](#); [Balakrishnan et al.,](#)

2013). This method considers several density levels, $\lambda_1 < \dots < \lambda_K$, and computes the number of connected components for the upper density level set at each level. As we increase the density level, some connected components may vanish and others may split into additional components. In the typical case when the underlying density function is a Morse function (i.e., Hessian at critical points is non-degenerate) (Morse, 1925, 1930; Milnor, 1963), the connected component disappears when the density level is above the maximum density value over the component and splits only if the density level passes the density value of some saddle points within the component (Klemelä, 2009). The vanishing and splitting of components as the level changes produces a tree structure. The density tree uses this tree structure as a visualization of the level sets. We refer to Klemelä (2009) for more details.

Density trees display primarily topological information about the underlying density function (Stuetzle, 2003; Kent et al., 2013) but need not preserve or impart other features that may be of interest. Extensions have been proposed that would endow the tree with additional information about the distribution (Klemelä, 2004, 2006, 2009), but this is difficult to do with multiple features and can make the visualization difficult to interpret. See Figure 8 for an example.

In this section, we propose a novel technique that visualizes several density (upper) level sets that preserve some geometric information and that are very easy to understand. Our method is based on the relationship between level set clustering and mode clustering (see Figure 9). Note that in this section, we will focus on density upper level sets.

Our method complements existing tree-based methods. It combine two clustering techniques – level-set and mode clustering – to produce a simple and intuitive visualization.

5.1 Mode Clustering and Density Upper Level Sets

Mode clustering (in particular, the method known as mean-shift clustering) was introduced in Fukunaga and Hostetler (1975), where data points are clustered by following the gradient flows of the kernel density estimator from each point to a local mode. The clusters are the “basins of attraction” of each local mode (Fukunaga and Hostetler, 1975; Cheng, 1995; Comaniciu and Meer, 2002). More generally, given a smooth Morse function p , mode clustering works as follows (Li et al., 2007; Chacón, 2012; Chen et al., 2014c). We form a partition of \mathbb{K} based on the gradient field $g \equiv \nabla p$.

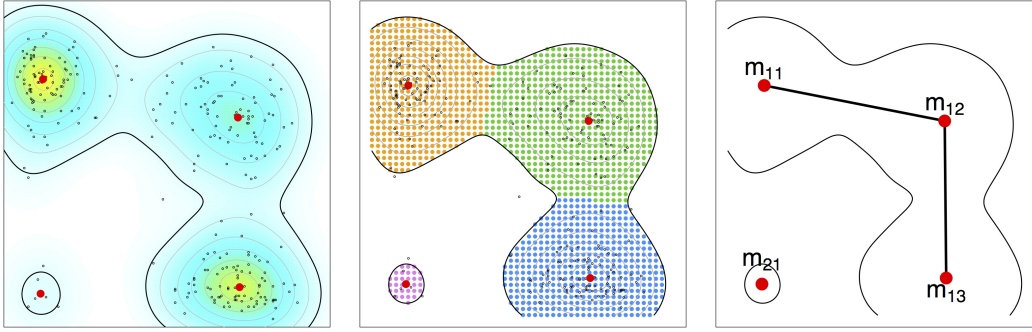


Figure 9: An example for density level set and mode clustering. Left: density level set (thick black contour denotes the specified level); four red dots are the local modes. Middle: basins of attraction for each local modes intersecting the density level set. Right: graph representation. There are two connected components. The large connected components contain three local modes $m_{1,1}, m_{1,2}, m_{1,3}$ with $m_{1,1}, m_{1,2}$ and $m_{1,2}, m_{1,3}$ are connected.

For each $x \in \mathbb{K}$, we define a gradient flow $\pi_x : [0, \infty) \mapsto \mathbb{K}$:

$$\pi_x(0) = x, \quad \pi'_x(t) = g(\pi_x(t)). \quad (45)$$

That is, $\pi_x(t)$ starts at x and moves along the gradient of p . We define the destination for $\pi_x(t)$ as $\mathbf{dest}(x) = \lim_{t \rightarrow \infty} \pi_x(t)$. Let \mathcal{M} be the collection of all local modes of p . It can be shown that $\mathbf{dest}(x) \in \mathcal{M}$ except for a set of x 's in a set \mathcal{B} with Lebesgue measure 0 (this set corresponds to the boundaries of clusters). For each mode $m_j \in \mathcal{M}$, we define its basin of attraction as

$$\mathcal{A}_j = \{x \in \mathbb{K} : \mathbf{dest}(x) = m_j\}. \quad (46)$$

The regions $\mathcal{A}_1, \dots, \mathcal{A}_k$ are the clusters generated by mode clustering.

Now we recall three facts about an upper density level set $L = \{x : p(x) \geq \lambda\}$ (c.f. Figure 9 left and middle panels):

1. L can be decomposed into connected components $L = \bigcup_{\ell=1}^K \mathcal{C}_\ell$, where the \mathcal{C}_ℓ are disjoint, connected compact sets under regularity conditions.
2. Each \mathcal{C}_ℓ contains at least one local mode.
3. If \mathcal{C}_ℓ contains s local modes, then $\mathcal{C}_\ell = \mathcal{C}_{\ell,1}^\lambda \cup \dots \cup \mathcal{C}_{\ell,s}^\lambda \cup \mathcal{B}$, where $\mathcal{C}_{\ell,j}^\lambda$ is the basin of attraction for a local mode $m_{\ell,j}$ intersected with the level set L and \mathcal{B} are the boundaries of the basins which has 0 Lebesgue measure. Namely, $\mathcal{C}_{\ell,j}^\lambda = L \cap \mathcal{A}_k$ for some k .

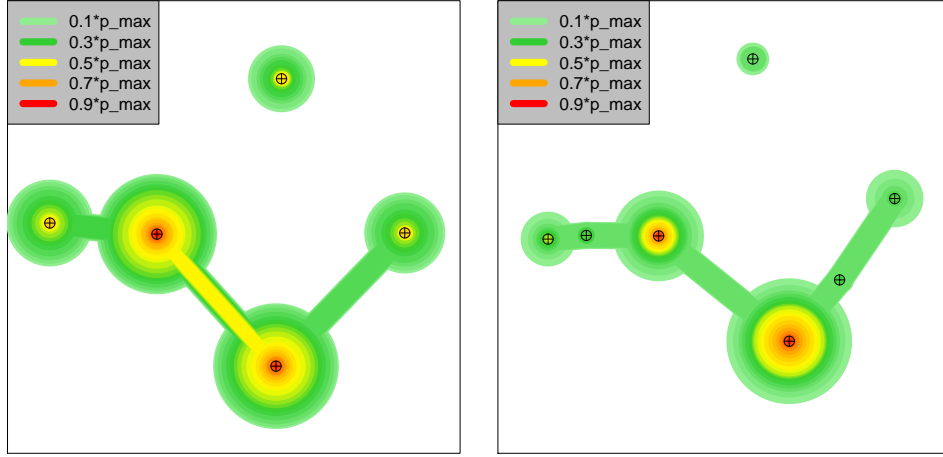


Figure 10: A visualization example in multivariate cases. We use the same dataset as Figure 8 but add an additional Gaussian noise to each data point to make it a higher dimensional dataset. Left: a 6 dimensional dataset (add 3 additional dimensional noises). Right: a 10 dimensional dataset (add 7 additional dimensional noises).

Thus, the upper level sets are covered by the basins of attraction of the local modes (the uncovered regions have Lebesgue measure 0 so we ignore them for visualization).

We then create a graph $G = (V, E)$ with each node corresponding to a local mode within L_h and each edge representing a *connection* between local modes to represent a level set. Specifically, we add an edge to a pair of local modes $(m_{\ell,j}, m_{\ell,k})$ when the corresponding basins $\mathcal{C}_{\ell,j}^\lambda$ and $\mathcal{C}_{\ell,k}^\lambda$ shares the same boundaries. i.e. $\bar{\mathcal{C}}_{\ell,j}^\lambda \cap \bar{\mathcal{C}}_{\ell,k}^\lambda \neq \phi$. Two local modes have an edge only if they are in the same connected component and their shared boundaries are also in the upper level set. Figure 9 provides an example illustrating these parts.

5.2 Visualization Algorithm

We construct visualization using Algorithm 1. First, we perform mode clustering to obtain local modes $m_1, \dots, m_k \in \mathbb{R}^d$. We use the mean shift algorithm (Fukunaga and Hostetler, 1975; Cheng, 1995; Comaniciu and Meer, 2002) to find the modes of density estimate. Second, we perform multidimensional scaling (MDS; Kruskal 1964) to all the modes to map them onto a 2D plane. Let $m_1^\dagger, \dots, m_k^\dagger \in \mathbb{R}^2$ be the corresponding locations after MDS. Third, we assign local mode m_ℓ an index

$$r_\ell(\lambda) = \frac{n_\ell(\lambda)}{n}, \quad n_\ell(\lambda) = \sum_{i=1}^n 1 \left(\widehat{\text{dest}}(X_i) = m_\ell \wedge \widehat{p}_h(X_i) \geq \lambda \right), \quad (47)$$

where $n_\ell(\lambda)$ is the number of data points that are assigned to m_ℓ by mode clustering and have (estimated) density being greater or equal to λ . Fourth, if $r_\ell(\lambda) > 0$, we create a circle around each m_ℓ^\dagger with radius proportional to $r_\ell(\lambda)$. If $r_\ell(\lambda) = 0$, we ignore this local mode; this occurs if the (estimated) density of the mode (and its basin of attractions) lies below λ . Fifth, we connect two local modes m_ℓ^\dagger and m_j^\dagger if they belong to the same connected component of the estimated upper level set $\widehat{L}_h = \{x : \widehat{p}_h(x) \geq \lambda\}$ and their basins of attraction intersect \widehat{L}_h share the same boundary (see e.g. Figure 9 middle and right panel). Note that this step might be computationally difficult in practice. An efficient alternative is to examine the shortest distance between two connected components; if the distance is sufficiently small, we claim these two components share the same boundary. Finally, we set the width of the line connecting m_ℓ and m_j to be proportional to $r_\ell(\lambda) + r_j(\lambda)$.

Given several density levels, $\lambda_1 < \dots < \lambda_K$, we can overlay the visualization from the previous paragraph from λ_1 to λ_K to create a “tomographic” visualization of the clusters. This gives a visualization for the density level sets. Figure 10 shows an example for visualizing level sets for a 6-dimensional and a 10-dimensional simulation datasets at different density levels. This dataset is from [Chen et al. \(2014c\)](#).

Algorithm 1 Visualization for a single level set

Input: Data $\{X_1, \dots, X_n\}$, density level λ , smoothing parameter h

1. Compute the kernel density estimator \widehat{p}_h .
2. Find the modes m_1, \dots, m_k of \widehat{p}_h (one can apply the mean shift algorithm).
3. Apply multidimensional scaling to the modes to project them into \mathbb{R}^2 ; denote the corresponding locations as $m_1^\dagger, \dots, m_k^\dagger$.
4. For each local modes m_ℓ , we assign it an index (47)

$$r_\ell(\lambda) = \frac{n_\ell(\lambda)}{n}, \quad n_\ell(\lambda) = \sum_{i=1}^n 1 \left(\widehat{\text{dest}}(X_i) = m_\ell \wedge \widehat{p}_h(X_i) \geq \lambda \right).$$

5. If $r_\ell(\lambda) > 0$, we create a circle around m_ℓ^\dagger with radius in proportional to $r_\ell(\lambda)$.
 6. We connect two local modes m_ℓ^\dagger and m_j^\dagger if
 - (1) they belong to the same connected component of \widehat{L}_h , the estimated upper level set at level λ , and
 - (2) their basins of attraction above level set share the same boundary.
 7. Adjust the width for the line connecting m_ℓ^\dagger and m_j^\dagger to be in proportion to $r_\ell(\lambda) + r_j(\lambda)$.
-

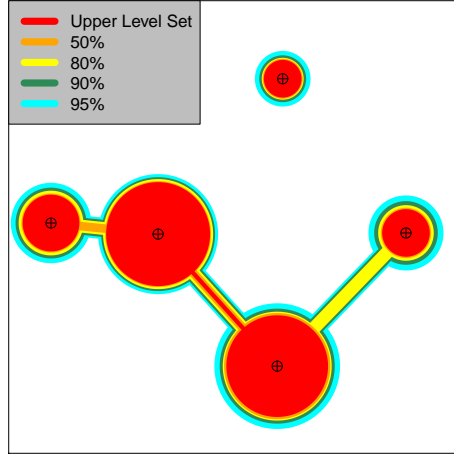


Figure 11: A visualization for confidence sets of an upper set with level λ . This is the 6 dimensional dataset of Figure 10. We pick the density level $\lambda = 0.4 \times \sup_x \|\widehat{p}_h(x)\|$ and display confidence levels under $\alpha = (50\%, 80\%, 90\%, 95\%)$.

5.3 Visualizing Level Sets with Confidence

A modified version of our algorithm allows us to visualize multivariate confidence sets for an upper level set at a given level λ . In particular, we visualize the confidence set for the level sets produced by Method 2 (supremum loss, see Section 4.2). The advantage of Method 2 here is that this confidence set under different α 's is just the density level set at different λ 's. This makes it easy to visualize K distinct confidence sets for pre-specified levels $\alpha_1 < \dots < \alpha_K$.

Recall that $\widehat{M}_n^* = \sup_{x \in \mathbb{K}} |\widehat{p}_h^*(x) - \widehat{p}_h(x)|$ is the bootstrap supremum deviation for the KDE and $\widehat{m}_{1-\alpha} = F_{M_n^*}^{-1}(1 - \alpha)$ is the quantile. When we want to visualize confidence sets for the upper level set L_h at different significance levels, we pick

$$\lambda_1 = \lambda - \widehat{m}_{1-\alpha_1}, \dots, \lambda_K = \lambda - \widehat{m}_{1-\alpha_K} \quad (48)$$

and use the visualization algorithm to create a tomographic visualization. Figure 11 provides an example for visualizing confidence sets for upper level set using the 6 dimensional simulation data in Figure 10.

Remark 7. At the cost of additional computation, we can also use Method 1 (Hausdorff loss) instead of Method 2, combining it with the basins of attractions to visualize the confidence sets. We use method 1 to construct the inner/outer confidence sets and then we find the connected components and partition it by the basins of attraction for local modes and use multidimensional scaling to visualize it in low dimensions.

6 Discussion

In this paper, we derived the limiting distribution for smoothed density level sets under Hausdorff loss. This result immediately allows us to construct confidence sets for the smoothed level set. We developed two bootstrapping methods to construct the confidence sets, and we showed that both methods are consistent. These confidence sets can be inverted to construct multiple local tests of whether a point's density value is above or below a given level, which has application to related problems such as anomaly detection. Finally, we developed a new visualization method that is informative and interpretable, even in multidimensions.

Although we focused on density level sets in this paper, our methods, including confidence sets and visualization, can be applied to a more general class of problems such as kernel classifier, two-sample tests, and generalized level sets (See [Mammen and Polonik 2013](#) for more details.).

References

- S. Balakrishnan, S. Narayanan, A. Rinaldo, A. Singh, and L. Wasserman. Cluster trees on manifolds. In *Advances in Neural Information Processing Systems*, pages 2679–2687, 2013.
- Y. Benjamini and Y. Hochberg. Controlling the false discovery rate: a practical and powerful approach to multiple testing. *Journal of the Royal Statistical Society. Series B (Methodological)*, pages 289–300, 1995.
- M. M. Breunig, H.-P. Kriegel, R. T. Ng, and J. Sander. Lof: identifying density-based local outliers. In *ACM sigmod record*, volume 29, pages 93–104. ACM, 2000.
- B. Cadre. Kernel estimation of density level sets. *Journal of multivariate analysis*, 97(4):999–1023, 2006.
- B. Cadre, B. Pelletier, and P. Pudlo. Clustering by estimation of density level sets at a fixed probability, 2009.
- J. E. Chacón. Clusters and water flows: a novel approach to modal clustering through morse theory. *arXiv preprint arXiv:1212.1384*, 2012.

- V. Chandola, A. Banerjee, and V. Kumar. Anomaly detection: A survey. *ACM Computing Surveys (CSUR)*, 41(3):15, 2009.
- P. Chaudhuri and J. S. Marron. Sizer for exploration of structures in curves. *Journal of the American Statistical Association*, 94(447):807–823, 1999.
- P. Chaudhuri, J. Marron, et al. Scale space view of curve estimation. *The Annals of Statistics*, 28(2):408–428, 2000.
- F. Chazal and A. Lieutier. The “ λ -medial axis”. *Graphical Models*, 67(4):304–331, 2005.
- F. Chazal, A. Lieutier, and J. Rossignac. Normal-map between normal-compatible manifolds. *International Journal of Computational Geometry & Applications*, 17(05):403–421, 2007.
- F. Chazal, D. Cohen-Steiner, and A. . Lieutier. A sampling theory for compact sets in euclidean space. *Discrete Computational Geometry*, 2009.
- Y.-C. Chen, C. R. Genovese, R. J. Tibshirani, and L. Wasserman. Nonparametric modal regression. *arXiv preprint arXiv:1412.1716*, 2014a.
- Y.-C. Chen, C. R. Genovese, and L. Wasserman. Asymptotic theory for density ridges. *arXiv preprint arXiv:1406.5663*, 2014b.
- Y.-C. Chen, C. R. Genovese, and L. Wasserman. Enhanced mode clustering. *arXiv preprint arXiv:1406.1780*, 2014c.
- Y. Cheng. Mean shift, mode seeking, and clustering. *Pattern Analysis and Machine Intelligence, IEEE Transactions on*, 17(8):790–799, 1995.
- V. Chernozhukov, E. Kocatulum, and K. Menzel. Inference on sets in finance. *arXiv preprint arXiv:1211.4282*, 2012.
- V. Chernozhukov, D. Chetverikov, and K. Kato. Anti-concentration and honest, adaptive confidence bands. *The Annals of Statistics*, 42(5):1787–1818, 2014a.
- V. Chernozhukov, D. Chetverikov, and K. Kato. Comparison and anti-concentration bounds for maxima of gaussian random vectors. *Probability Theory and Related Fields*, pages 1–24, 2014b.

- V. Chernozhukov, D. Chetverikov, and K. Kato. Gaussian approximation of suprema of empirical processes. *The Annals of Statistics*, 42(4):1564–1597, 2014c.
- V. Chernozhukov, D. Chetverikov, and K. Kato. Central limit theorems and bootstrap in high dimensions. *arXiv preprint arXiv:1412.3661*, 2014.
- D. Comaniciu and P. Meer. Mean shift: A robust approach toward feature space analysis. *Pattern Analysis and Machine Intelligence, IEEE Transactions on*, 24(5):603–619, 2002.
- A. Cuevas. Set estimation: Another bridge between statistics and geometry. *Boletín de Estadística e Investigación Operativa*, 25(2):71–85, 2009.
- A. Cuevas and A. Rodríguez-Casal. On boundary estimation. *Advances in Applied Probability*, pages 340–354, 2004.
- A. Cuevas, W. González-Manteiga, and A. Rodríguez-Casal. Plug-in estimation of general level sets. *Australian & New Zealand Journal of Statistics*, 48(1):7–19, 2006.
- A. Cuevas, R. Fraiman, and B. Pateiro-López. On statistical properties of sets fulfilling rolling-type conditions. *Advances in Applied Probability*, 44(2):311–329, 2012.
- M. Desforges, P. Jacob, and J. Cooper. Applications of probability density estimation to the detection of abnormal conditions in engineering. *Proceedings of the Institution of Mechanical Engineers, Part C: Journal of Mechanical Engineering Science*, 212(8):687–703, 1998.
- T. Duong, I. Koch, and M. Wand. Highest density difference region estimation with application to flow cytometric data. *Biometrical Journal*, 51(3):504–521, 2009.
- U. Einmahl and D. M. Mason. Uniform in bandwidth consistency of kernel-type function estimators. *The Annals of Statistics*, 33(3):1380–1403, 2005.
- H. Federer. Curvature measures. *Transactions of the American Mathematical Society*, pages 418–491, 1959.
- K. Fukunaga and L. Hostetler. The estimation of the gradient of a density function, with applications in pattern recognition. *Information Theory, IEEE Transactions on*, 21(1):32–40, 1975.

- C. R. Genovese, M. Perone-Pacifco, I. Verdinelli, and L. Wasserman. Nonparametric ridge estimation. *The Annals of Statistics*, 42(4):1511–1545, 2014.
- E. Giné and A. Guillaou. Rates of strong uniform consistency for multivariate kernel density estimators. In *Annales de l'Institut Henri Poincaré (B) Probability and Statistics*, volume 38, pages 907–921. Elsevier, 2002.
- F. Godtlielsen, J. Marron, and P. Chaudhuri. Significance in scale space for bivariate density estimation. *Journal of Computational and Graphical Statistics*, 11(1):1–21, 2002.
- J. A. Hartigan. Clustering algorithms. *Wiley series in probability and mathematical statistics. 25 cm. 351 p.*, 1975.
- Z. He, X. Xu, and S. Deng. Discovering cluster-based local outliers. *Pattern Recognition Letters*, 24(9):1641–1650, 2003.
- V. J. Hodge and J. Austin. A survey of outlier detection methodologies. *Artificial Intelligence Review*, 22(2):85–126, 2004.
- H. Jankowski and L. Stanberry. Confidence regions in level set estimation. *Preprint*, 2012.
- B. P. Kent, A. Rinaldo, and T. Verstynen. Debacl: A python package for interactive density-based clustering. *arXiv preprint arXiv:1307.8136*, 2013.
- J. Klemelä. Visualization of multivariate density estimates with level set trees. *Journal of Computational and Graphical Statistics*, 13(3), 2004.
- J. Klemelä. Visualization of multivariate density estimates with shape trees. *Journal of Computational and Graphical Statistics*, 15(2):372–397, 2006.
- J. Klemelä. *Smoothing of multivariate data: density estimation and visualization*, volume 737. John Wiley & Sons, 2009.
- J. B. Kruskal. Multidimensional scaling by optimizing goodness of fit to a nonmetric hypothesis. *Psychometrika*, 29(1):1–27, 1964.
- T. Laloe and R. Servien. Nonparametric estimation of regression level sets. *Journal of the Korean Statistical Society*, 2013.

- J. Li, S. Ray, and B. G. Lindsay. A nonparametric statistical approach to clustering via mode identification. *Journal of Machine Learning Research*, 8(8):1687–1723, 2007.
- E. Mammen and W. Polonik. Confidence regions for level sets. *Journal of Multivariate Analysis*, 122:202–214, 2013.
- E. Mammen and A. B. Tsybakov. Smooth discrimination analysis. *The Annals of Statistics*, 27(6):1808–1829, 1999.
- D. M. Mason and W. Polonik. Asymptotic normality of plug-in level set estimates. *The Annals of Applied Probability*, 19(3):1108–1142, 2009.
- J. W. Milnor. *Morse theory*. Number 51. Princeton university press, 1963.
- I. Molchanov. Empirical estimation of distribution quantiles of random closed sets. *Theory of Probability & Its Applications*, 35(3):594–600, 1991.
- I. Molchanov. *Theory of random sets*. Springer-Verlag London Ltd., 2005.
- I. S. Molchanov. A limit theorem for solutions of inequalities. *Scandinavian Journal of Statistics*, 25(1):235–242, 1998.
- M. Morse. Relations between the critical points of a real function of n independent variables. *Transactions of the American Mathematical Society*, 27(3):345–396, 1925.
- M. Morse. The foundations of a theory of the calculus of variations in the large in m -space (second paper). *Transactions of the American Mathematical Society*, 32(4):599–631, 1930.
- M. H. Neumann. Strong approximation of density estimators from weakly dependent observations by density estimators from independent observations. *Annals of Statistics*, pages 2014–2048, 1998.
- P. Niyogi, S. Smale, and S. Weinberger. Finding the homology of submanifolds with high confidence from random samples. *Discrete & Computational Geometry*, 39(1-3):419–441, 2008.
- B. Pateiro-López. *Set estimation under convexity type restrictions*. PhD thesis, UNIVERSIDADE DE SANTIAGO DE COMPOSTELA, 2008.

- W. Polonik. Measuring mass concentrations and estimating density contour clusters—an excess mass approach. *The Annals of Statistics*, pages 855–881, 1995.
- A. Rinaldo and L. Wasserman. Generalized density clustering. *The Annals of Statistics*, 38(5):2678–2722, 2010.
- A. Rinaldo, A. Singh, R. Nugent, and L. Wasserman. Stability of density-based clustering. *The Journal of Machine Learning Research*, 13(1):905–948, 2012.
- B. W. Silverman. *Density Estimation for Statistics and Data Analysis*. Chapman and Hall, 1986.
- A. Singh, C. Scott, and R. Nowak. Adaptive hausdorff estimation of density level sets. *The Annals of Statistics*, 37(5B):2760–2782, 2009.
- W. Stuetzle. Estimating the cluster tree of a density by analyzing the minimal spanning tree of a sample. *Journal of classification*, 20(1):025–047, 2003.
- W. Stuetzle and R. Nugent. A generalized single linkage method for estimating the cluster tree of a density. *Journal of Computational and Graphical Statistics*, 19(2), 2010.
- A. B. Tsybakov. On nonparametric estimation of density level sets. *The Annals of Statistics*, 25(3):948–969, 1997.
- A. W. Van Der Vaart and J. A. Wellner. *Weak Convergence*. Springer, New York, 1996.
- G. Walther. Granulometric smoothing. *The Annals of Statistics*, 25(6):2273–2299, 1997.
- L. Wasserman. *All of Nonparametric Statistics*. Springer-Verlag New York, Inc., 2006.

7 Proofs

Theorem 8 (Theorem 2 in Cuevas et al. (2006)). *Assume (K1–2) and (G), then we have*

$$\text{Haus}(\widehat{D}_h, D_h) = O(\|\widehat{p}_h - p_h\|_{0,\max}).$$

Theorem 9 (Talagrand’s inequality; version of Theorem 12 in [Chen et al. \(2014a\)](#)). Assume (K1–2), then for each $t > 0$ there exists some n_0 such that whenever $n > n_0$, we have

$$\mathbb{P}(\|\widehat{p}_h - p_h\|_{\ell, \max}^* > t) \leq (\ell + 1)e^{-tnh^{d+2\ell}A_1},$$

for some constant A_1 and $\ell = 0, 1, 2$. Moreover,

$$\mathbb{E}(\|\widehat{p}_h - p_h\|_{2, \max}^*) = O\left(\sqrt{\frac{\log n}{nh^{d+4}}}\right).$$

PROOF FOR LEMMA 1. We first prove the lower bound for $\text{reach}(D_h)$ and then we will prove the additional assertions.

Part 1: Lower bound on reach. We prove this by contradiction. Take x near D_h such that

$$d(x, D_h) < \left(\frac{\delta_0}{2}, \frac{g_0}{\|p_h\|_{2, \max}^*}\right). \quad (49)$$

We assume that x has two projections onto D_h , denoted as b and c .

Since $b, c \in D_h$, $p_h(b) - \lambda = p_h(c) - \lambda = 0$ so that $p_h(b) - p_h(c) = 0$. Now by Taylor’s theorem

$$\begin{aligned} \|(b - c)^T \nabla p_h(b)\| &= \|p_h(b) - p_h(c) - (b - c)^T \nabla p_h(b)\| \\ &\leq \frac{1}{2} \|b - c\|^2 \|p_h\|_{2, \max}. \end{aligned} \quad (50)$$

By the definition of projection, we can find a constant $t_b \in \mathbb{R}$ such that $x - b = t_b \nabla p_h(b)$. Together with (50),

$$\begin{aligned} 2|(b - c)^T(x - b)| &= 2|(b - c)^T \nabla p_h(b) t_b| \\ &\leq \|(b - c)^T \nabla p_h(b)\| |t_b| \\ &\leq \|p_h\|_{2, \max} \|b - c\|^2 |t_b|. \end{aligned} \quad (51)$$

Since both b and c are projection points from x onto D_h ,

$$\|x - b\| = \|x - c\|.$$

Thus, we have

$$\begin{aligned}
0 &= \|x - c\|^2 - \|x - b\|^2 \\
&= \|b - c\|^2 + 2(b - c)^T(x - b) \\
&\geq \|b - c\|^2 - \|p_h\|_{2,\max} \|b - c\|^2 |t_b| \\
&= \|b - c\|^2 (1 - \|p_h\|_{2,\max} |t_b|).
\end{aligned} \tag{52}$$

Recall that $d(x, D_h) \leq \frac{g_0}{\|p_h\|_{2,\max}}$ and by Taylor's theorem,

$$\frac{g_0}{\|p_h\|_{2,\max}} > d(x, D_h) = \|x - b\| = \|t_b \nabla p_h(b)\| = |t_b| \|\nabla p_h(b)\| \geq |t_b| g_0 \tag{53}$$

so that $|t_b| \|p_h\|_{2,\max} < 1$. Note that the lower bound g_0 in the last inequality is because $d(x, D_h) < \frac{\delta_0}{2}$ so it follows from assumption (G). Plugging in this result into the last equality of (52), we conclude that $\|b - c\| = 0$. This shows $b = c$ so that we have a unique projection. Thus, whenever $d(x, D_h) < \left(\frac{\delta_0}{2}, \frac{g_0}{\|p_h\|_{2,\max}^*}\right)$, we have a unique projection onto D_h and thus we have proved the lower bound on reach.

Part 2: The three assertions. The first assertion is trivially true when $\|p_h - q\|_{2,\max}^*$ is sufficiently small since assumption (G) only involves gradients (first derivatives).

The second assertion follows from the lower bound on reach. By assertion 1, (G) holds for q . And the lower bound on reach is bounded by gradient and second derivatives so that we have the prescribed bound.

The third assertion follows from Theorem 1 in Chazal et al. (2007) which states that if two $d - 1$ dimensional smooth manifolds M_1 and M_2 have Hausdorff distance being less than $(2 - \sqrt{2}) \min\{\text{reach}(M_1), \text{reach}(M_2)\}$, then M_1 and M_2 are normal compatible to each other. Now by Theorem 8, the Hausdorff distance between D_h and $D(q)$ is at rate $O(\|p_h - q\|_{1,\max})$ so that this assertion is true when $\|p_h - q\|_{2,\max}$ is sufficiently small. \square

PROOF OF LEMMA 2. Let $x \in D_h$. We define $\Pi(x) \in D_h$ to be the projected point onto \widehat{D}_h . By Lemma 1 and Theorem 8, when $\|\widehat{p}_h - p_h\|_{2,\max}^* \rightarrow 0$, $\text{Haus}(D_h, \widehat{D}_h) \xrightarrow{P} 0$ so that $\Pi(x)$ is unique. Thus, we assume $\Pi(x)$ is unique.

Now since $\Pi(x) \in \widehat{D}_h$ and $x \in D_h$, $\widehat{p}_h(\Pi(x)) - p_h(x) = 0$. Thus, by Taylor's

theorem

$$\begin{aligned}\widehat{p}_h(x) - p_h(x) &= \widehat{p}_h(x) - \widehat{p}_h(\Pi(x)) \\ &= (x - \Pi(x))^T (\nabla \widehat{p}_h(\Pi(x)) + O_{\mathbb{P}}(\|x - \Pi(x)\|)).\end{aligned}\tag{54}$$

Note that $x - \Pi(x)$ is normal to \widehat{D}_h at $\Pi(x)$ so that it points toward the same direction as $\nabla \widehat{p}_h(\Pi(x))$. Thus, (54) can be rewritten as

$$\widehat{p}_h(x) - p_h(x) = \|x - \Pi(x)\| (\|\nabla \widehat{p}_h(\Pi(x))\| + O_{\mathbb{P}}(\|x - \Pi(x)\|)).\tag{55}$$

By Taylor's theorem, $\nabla \widehat{p}_h(\Pi(x))$ is close to $\nabla p_h(x)$ in the sense that

$$\nabla \widehat{p}_h(\Pi(x)) = \nabla p_h(x) + O(\|\widehat{p}_h - p_h\|_{1,\max}^*).\tag{56}$$

In addition, $O(\|x - \Pi(x)\|)$ is bounded by $O(\text{Haus}(\widehat{D}_h, D_h))$ which is at rate $O(\|\widehat{p}_h - p_h\|_{1,\max}^*)$ due to Theorem 8. Putting this together with (55), we conclude

$$\begin{aligned}\widehat{p}_h(x) - p_h(x) &= \|x - \Pi(x)\| (\|p_h(x)\| + O(\|\widehat{p}_h - p_h\|_{1,\max}^*)) \\ &= d(x, \widehat{D}_h) (\|p_h(x)\| + O(\|\widehat{p}_h - p_h\|_{1,\max}^*)).\end{aligned}\tag{57}$$

Note that the left hand side can be written as

$$\widehat{p}_h(x) - p_h(x) = \frac{1}{nh^d} \sum_{i=1}^n K\left(\frac{x - X_i}{h}\right) - \frac{1}{h^d} \mathbb{E}\left(K\left(\frac{x - X_i}{h}\right)\right) = \frac{1}{\sqrt{nh^d}} \mathbb{G}_n(\tilde{f}_x),\tag{58}$$

where $\tilde{f}_x(y) = K\left(\frac{x-y}{h}\right)$. After plugging (58) into the left hand side of (57), dividing both side by $\|p_h(x)\|$ and setting $f_x(y) = \frac{\tilde{f}_x(y)}{\sqrt{h^d}\|p_h(x)\|}$, we obtain

$$\frac{\frac{1}{\sqrt{nh^d}} \mathbb{G}_n(f_x) - d(x, \widehat{D}_h)}{d(x, \widehat{D}_h)} = O(\|\widehat{p}_h - p_h\|_{1,\max}^*).\tag{59}$$

This holds uniformly for all $x \in D_h$ and note that the definition of \mathcal{F} is

$$\mathcal{F} = \left\{ f_x(y) \equiv \frac{1}{\sqrt{h^d}\|\nabla p_h(x)\|} K\left(\frac{x-y}{h}\right) : x \in D_h \right\}.$$

So we conclude

$$\sup_{x \in D_h} \left| \frac{\frac{1}{\sqrt{nh^d}} \mathbb{G}_n(f_x) - d(x, \widehat{D}_h)}{d(x, \widehat{D}_h)} \right| = O(\|\widehat{p}_h - p_h\|_{1, \max}^*).$$

□

PROOF FOR THEOREM 3. The proof for Theorem 3 follows the same procedure as the proof of Theorem 6 in [Chen et al. \(2014b\)](#). The proof contains two parts: Gaussian approximation and anti-concentration.

Part 1: Gaussian approximation. Basically, we will show that

$$\sqrt{nh^d} \text{Haus}(\widehat{D}_h, D_h) \approx \sup_{f \in \mathcal{F}} |\mathbb{G}_n(f)| \approx \sup_{f \in \mathcal{F}} |\mathbb{B}(f)|,$$

where \mathbb{B} is a Gaussian process defined in (13) of the original paper.

First, when $\|\widehat{p}_h - p_h\|$ is sufficiently small, \widehat{D}_h and D_h are normal compatible to each other by Lemma 1. Then by the property of normal compatible,

$$\sup_{x \in D_h} d(x, \widehat{D}_h) = \text{Haus}(\widehat{D}_h, D_h). \quad (60)$$

Thus, the difference

$$\begin{aligned} \left| \sqrt{nh^d} \text{Haus}(\widehat{D}_h, D_h) - \sup_{f \in \mathcal{F}} |\mathbb{G}_n(f)| \right| &= \left| \sqrt{nh^d} \sup_{x \in D_h} d(x, \widehat{D}_h) - \sup_{f \in \mathcal{F}} |\mathbb{G}_n(f)| \right| \\ &\leq \frac{\sup_{x \in D_h} \left| \frac{1}{\sqrt{nh^d}} \mathbb{G}_n(f_x) - d(x, \widehat{D}_h) \right|}{\frac{1}{\sqrt{nh^d}}} \\ &= \sup_{x \in D_h} \left| \frac{\frac{1}{\sqrt{nh^d}} \mathbb{G}_n(f_x) - d(x, \widehat{D}_h)}{d(x, \widehat{D}_h)} \right| O_{\mathbb{P}}(1) \\ &= O(\|\widehat{p}_h - p_h\|_{1, \max}^*). \end{aligned} \quad (61)$$

Note that the last two inequality follows from the fact that $d(x, \widehat{D}_h) \leq O_{\mathbb{P}}(\frac{1}{\sqrt{nh^d}})$. By Theorem 9 the above result implies,

$$\mathbb{P} \left(\left| \sqrt{nh^d} \text{Haus}(\widehat{D}_h, D_h) - \sup_{f \in \mathcal{F}} |\mathbb{G}_n(f)| \right| > t \right) \leq 2e^{-t^2 h^{d+2} A_2} \quad (62)$$

for some constant A_2 .

Now by Corollary 2.2 in [Chernozhukov et al. \(2014c\)](#), there exists some random

variable $\mathbf{B} \stackrel{d}{=} \sup_{f \in \mathcal{F}} |\mathbb{B}(f)|$ such that for all $\gamma \in (0, 1)$ and n is sufficiently large,

$$\mathbb{P} \left(\left| \sup_{f \in \mathcal{F}} |\mathbb{G}_n(f)| - \mathbf{B} \right| > A_3 \frac{\log^{2/3}(n)}{\gamma^{1/3}(nh^d)^{1/6}} \right) \leq A_4 \gamma. \quad (63)$$

Note that this result basically follows from the same derivation of Proposition 3.1 in Chernozhukov et al. (2014c) with the fact that $g \equiv 1$ in their definition.

Combining equations (62) and (63) and pick $t = 1/\sqrt{nh^{d+2}}$, we have that for n is sufficiently large and $\gamma \in (0, 1)$,

$$\mathbb{P} \left(\left| \sqrt{nh^d} \text{Haus}(\widehat{D}_h, D_h) - \mathbf{B} \right| > A_3 \frac{\log^{2/3}(n)}{\gamma^{1/3}(nh^d)^{1/6}} + \frac{1}{\sqrt{nh^{d+2}}} \right) \leq A_4 \gamma + 2e^{-\sqrt{nh^{d+2}} A_2}. \quad (64)$$

Part 2: Anti-concentration. To obtain the desired Berry-Esseen bound, we apply the anti-concentration inequality in Chernozhukov et al. (2014c) and Chernozhukov et al. (2014a).

Lemma 10 (Modification of Lemma 2.3 in Chernozhukov et al. (2014c)). *Let $\mathbf{B} \stackrel{d}{=} \sup_{f \in \mathcal{F}} |\mathbb{B}(f)|$, where \mathbb{B} and \mathcal{F} are defined as the above. Assume (K1-2) and that there exists a random variable Y such that $\mathbb{P}(|Y - \mathbf{B}| > \eta) < \delta(\eta)$. Then*

$$\sup_t |\mathbb{P}(Y < t) - \mathbb{P}(\mathbf{B} < t)| \leq A_5 \mathbb{E}(\mathbf{B}) \eta + \delta(\eta)$$

for some constant A_5 .

It is easy to verify that assumptions (K1-2) imply the assumptions (A1-3) in Chernozhukov et al. (2014c) so that the result follows. Note that in the original Lemma 2.3 in Chernozhukov et al. (2014c), $\mathbb{E}(\mathbf{B})$ should be replaced by $\mathbb{E}(\mathbf{B}) + \log \eta$. However, $\mathbb{E}(\mathbf{B}) = O(\sqrt{\log n})$ due to Dudley's inequality for Gaussian process (Van Der Vaart and Wellner, 1996) and later we will find that $\log \eta$ is also at this rate so we ignore $\log \eta$.

From Lemma 10 and equation (64), there exists some constant A_6 such that

$$\begin{aligned} \sup_t \left| \mathbb{P} \left(\sqrt{nh^d} \text{Haus}(\widehat{D}_h, D_h) < t \right) - \mathbb{P} \left(\sup_{f \in \mathcal{F}} |\mathbb{B}(f)| < t \right) \right| \\ \leq A_5 \mathbb{E}(\mathbf{B}) \left(A_3 \frac{\log^{2/3}(n)}{\gamma^{1/3}(nh^d)^{1/6}} + \frac{1}{\sqrt{nh^{d+2}}} \right) + A_4 \gamma + 2e^{-\sqrt{nh^{d+2}}A_2} \quad (65) \\ \leq A_6 \left(A_3 \frac{\log^{7/6}(n)}{\gamma^{1/3}(nh^d)^{1/6}} + \sqrt{\frac{\log n}{nh^{d+2}}} \right) + A_4 \gamma + 2e^{-\sqrt{nh^{d+2}}A_2}. \end{aligned}$$

Now pick $\gamma = \left(\frac{\log^7 n}{nh^d} \right)^{1/8}$ and use the fact that $\frac{1}{\sqrt{nh^{d+2}}}$ and $2e^{-\sqrt{nh^{d+2}}A_2}$ converges faster than the other terms; we obtain the desired rate. \square

PROOF FOR THEOREM 4. This proof follows the same strategy for the proof of Theorem 7 in Chen et al. (2014b). We prove the Berry-Esseen type bound first and then show that the coverage is consistent. We prove the Berry-Esseen bound in two simple steps: Gaussian approximation and support approximation.

Let $\mathcal{X}_n = \{(X_1, \dots, X_n) : \|\widehat{p}_h - p_h\|_{2, \max}^* \leq \eta_0\}$ for some small η_0 so that whenever our data is within \mathcal{X}_n , (G) holds for \widehat{p}_h . By Lemma 1, such an η_0 exists and by Theorem 9 we have $\mathbb{P}(\mathcal{X}_n) \geq 1 - 3^{-nh^{d+4}\tilde{A}_0}$ for some constant \tilde{A}_0 . Thus, we assume our original data X_1, \dots, X_n is within \mathcal{X}_n .

Step 1: Gaussian approximation. Let $\widehat{\mathbb{P}}_n$ and $\widehat{\mathbb{P}}_n^*$ be the empirical measure and the bootstrap empirical measure. A crucial observation is that for a function $f_x(y) = K\left(\frac{x-y}{h}\right)$,

$$\widehat{\mathbb{P}}_n(f_x) = \int K\left(\frac{x-y}{h}\right) d\widehat{\mathbb{P}}_n(y) = h^d \widehat{p}_h(x). \quad (66)$$

Also note

$$\widehat{\mathbb{P}}_n^*(f_x) = \int K\left(\frac{x-y}{h}\right) d\widehat{\mathbb{P}}_n^*(y) = h^d \widehat{p}_h^*(x). \quad (67)$$

Therefore, for the bootstrap empirical process $\mathbb{G}_n^* = \sqrt{n}(\widehat{\mathbb{P}}_n^* - \widehat{\mathbb{P}}_n)$,

$$\widehat{p}_h^*(x) - \widehat{p}_h(x) = \frac{1}{\sqrt{n}h^d} \mathbb{G}_n^*(f_x). \quad (68)$$

Thus, if we sample from \widehat{p}_h and consider estimating \widehat{p}_h by \widehat{p}_h^* , we are doing exactly the same procedure of estimating p_h by \widehat{p}_h . Therefore, Lemma 2 and Theorem 3 hold

for approximating $\text{Haus}(\widehat{D}_h^*, \widehat{D}_h)$ by a maxima for a Gaussian process. The difference is that the Gaussian process is defined on

$$\mathcal{F}_n = \left\{ f_x(y) \equiv \frac{1}{\sqrt{nh^d} \|\nabla \widehat{p}_h(x)\|} K\left(\frac{x-y}{h}\right) : x \in \widehat{D}_h \right\} \quad (69)$$

since the “parameter (level sets)” being estimated is \widehat{D}_h (the estimator is \widehat{D}_h^*). Note that \mathcal{F}_n is very similar to \mathcal{F} except the denominator is slightly different and the support \widehat{D}_h is also different from D_h . That is, we have

$$\begin{aligned} \sup_t \left| \mathbb{P} \left(\sqrt{nh^d} \text{Haus}(\widehat{D}_h^*, \widehat{D}_h) < t \mid X_1, \dots, X_n \right) \right. \\ \left. - \mathbb{P} \left(\sup_{f \in \mathcal{F}_n} |\mathbb{B}_n(f)| < t \mid X_1, \dots, X_n \right) \right| \leq O \left(\left(\frac{\log^7 n}{nh^d} \right)^{1/8} \right), \end{aligned} \quad (70)$$

where \mathbb{B}_n is a Gaussian process on \mathcal{F}_n such that for any $f_1, f_2 \in \mathcal{F}_n$,

$$\mathbb{E}(\mathbb{B}_n(f_1) \mid X_1, \dots, X_n) = 0, \quad \text{Cov}(\mathbb{B}_n(f_1), \mathbb{B}_n(f_2) \mid X_1, \dots, X_n) = \frac{1}{n} \sum_{i=1}^n f_1(X_i) f_2(X_i). \quad (71)$$

Step 2: Support approximation. In this step, we will show that

$$\sup_{f \in \mathcal{F}_n} |\mathbb{B}_n(f)| \approx \sup_{f \in \mathcal{F}} |\mathbb{B}_n(f)| \approx \sup_{f \in \mathcal{F}} |\mathbb{B}(f)|. \quad (72)$$

The first approximation can be shown by using the Gaussian comparison lemma (Theorem 2 in [Chernozhukov et al. \(2014b\)](#); also see Lemma 17 in [Chen et al. \(2014b\)](#)). We do the same thing as Step 3 in the proof of Theorem 8 in [Chen et al. \(2014b\)](#) so we omit the details. Essentially, given any $\epsilon > 0$, we can construct a pair of balanced ϵ -nets for both \mathcal{F} and \mathcal{F}_n , denoted as $\{g_1, \dots, g_K\}$ and $\{g_1^n, \dots, g_K^n\}$ so that $\max_j \|g_j - g_j^n\|_{\max}^* = O(\|\widehat{p}_h - p_h\|_{1, \max}^*)$. Then this ϵ -net leads to

$$\begin{aligned} \sup_t \left| \mathbb{P} \left(\sup_{f \in \mathcal{F}_n} |\mathbb{B}_n(f)| < t \mid X_1, \dots, X_n \right) \right. \\ \left. - \mathbb{P} \left(\sup_{f \in \mathcal{F}} |\mathbb{B}_n(f)| < t \mid X_1, \dots, X_n \right) \right| \leq O \left((\|\widehat{p}_h - p_h\|_{1, \max}^*)^{1/3} \right). \end{aligned} \quad (73)$$

The difference between $\sup_{f \in \mathcal{F}_n} |\mathbb{B}_n(f)|$ and $\sup_{f \in \mathcal{F}} |\mathbb{B}(f)|$ is small since the these two

Gaussian processes differ in their covariance but as $n \rightarrow \infty$, the covariances converges at rate $1/\sqrt{n}$ so that we can neglect the difference between them. Thus, combining (70) and (73) and the argument from previous paragraph, we conclude

$$\begin{aligned} \sup_t \left| \mathbb{P} \left(\sqrt{nh^d} \text{Haus}(\widehat{D}_h^*, \widehat{D}_h) < t \mid X_1, \dots, X_n \right) - \mathbb{P} \left(\sup_{f \in \mathcal{F}} |\mathbb{B}(f)| < t \right) \right| \\ \leq O \left(\left(\frac{\log^7 n}{nh^d} \right)^{1/8} \right) + O \left((\|\widehat{p}_h - p_h\|_{1, \max}^*)^{1/3} \right). \end{aligned} \quad (74)$$

Now comparing the above result to Theorem 3 and using the fact that the first big-O term dominates the second term (the first is of rate $-1/8$ for n but the second term is at rate $-1/6$ by Theorem 9), we conclude the result for first assertion.

For the coverage, let $W_n = \text{Haus}(\widehat{D}_h, D_h)$ and $w_{n,1-\alpha} = F_{W_n}^{-1}(1 - \alpha)$. Since $D_h \subset \widehat{D}_h \oplus \text{Haus}(\widehat{D}_h, D_h)$, we have

$$\mathbb{P}(D_h \subset \widehat{D}_h \oplus w_{n,1-\alpha}) = 1 - \alpha. \quad (75)$$

Now by the first assertion, the difference for $w_{n,1-\alpha}$ and the bootstrap estimate $w_{n,1-\alpha}^*$ differs at rate $O \left(\left(\frac{\log^7 n}{nh^d} \right)^{1/8} \right)$, which completes the proof.

□

—